

Reply to referee #1

We would like to thank the reviewer for his/her helpful comments which are shown in blue below. Our replies are in green.

This study provides a time series analysis by merging TES and IASI measurements over a ten-year period. The manuscript is well written and it is an interesting work which investigates a dedicated methodology for homogenizing two different datasets in order to study in the future long-term trends in tropospheric ozone. However, I do have one major concern related to the results presented in figures 7 and 8, which should be addressed before final publication.

Major comments:

My biggest concern is related to the time series you show in figures 7 and 8 (top panels for Eastern Asia). I do have doubts about the methodology you use when looking at the sharp decrease you obtain after 2011 which seems quite unrealistic and coincident with the change of TES observing strategy. Is it possible that the random distribution of IASI scenes in spring 2011 is biased due to reasons you evoke in p.31034, l.25? Did you over-sample the IASI data over a specific period of the month or part of the region, which could possibly explain such a change in the time series? I'm wandering to what extent the different sub-samples might affect the results. I would recommend to provide some more sample testing in order to get a feeling for the robustness of the time series.

Note that the fact that the change of TES observing strategy has no bearing on the sampling of IASI points in the regions of interest, since the IASI points used to construct the ROI time series are not co-located with TES points. The random distribution of IASI scenes in spring 2011 is not biased. We took care to avoid this situation. We have now provided additional clarification on this point in the manuscript, by adding/changing the following sentences: *Data gaps in the time series occur for several reasons. A data point for a whole month is removed if an instrument has missing data for more than a week for that given month or if the whole area of the ROI is not completely covered by an instrument due to cloud cover or missing orbits. Missing orbits can lead to biased sampling of the random number generator within the ROI of a given month. However, the data has been screened for this by looking at the number of satellite scenes per day used for calculating the monthly mean: If the number of satellite scenes for 3 or more consecutive days is twice as high as the average for the rest of the month, the monthly data points are removed as well. For all data points included in the time series, care was taken to ensure that the initial distribution is unbiased.*

In terms of the realism of the sharp drop, we have now added a figure showing ozone from sonde measurements from Hilo, Hawaii. The Hilo ozone sondes are a completely independent dataset from the IASI satellite-based ozone estimates. We note that a sharp drop is also observed in the sonde observations at that particular location, which is strongly influenced by outflow of free tropospheric air from Asia.

p. 31035, l.1-3: You discuss the results considering the confidence limit, but not the standard deviation while this metric is independent of the sample size. I would suggest to represent the standard deviation associated with the monthly mean on Fig.7 and Fig.8 (error bars). If the std is larger than the sharp drop-off in 2011 or larger than ~5ppb which corresponds to the trend approximated over 2011-2014, it means that the decrease in 2011 or the increase since 2011 in Fig.8 might not be significant.

The standard deviation on the monthly means includes natural variability within a given month, within the domain of the ROI. The standard deviation on the monthly means is around 15 ppb. We agree that this number should be stated and have now added this information to the text.

15 ppb is indeed larger than the magnitude of the sharp drop off. However, we do not agree that the standard deviation is the most appropriate metric to assess the significance of the sharp drop. The significance of the calculated mean is clearly dependent on the sample size in this case, and therefore we maintain that the confidence limit is hence a more appropriate metric.

In addition, I'm also wandering in what way the offset values determined from the global measurement is suitable for the ROIs. If relevant, I would also recommend to provide IASI-TES frequency distribution panels for the ROIs.

Since the IASI and TES measurements for the ROIs presented in Figures 7 and 8 are not collocated, calculating a frequency distribution of the differences for the ROIs is not possible. The rationale for not co-locating the measurements for the ROIs is stated on p. 31033, l. 7-13.

We added to the manuscript a discussion about the width of the frequency distribution in Fig. 3. The width of the distribution can be explained with the precision of the instruments and the spatial and temporal collocation error only. The globally derived offset is valid for the ROIs since the most significant settings for the retrievals are identical (algorithm, a priori profiles, covariance matrices, see p. 31029, l. 21-23) and the offset is determined by the instrumental spectral resolution, i.e. weighting functions only. However, we added a table with Gaussian fit parameters for the global surveys split into individual seasons and latitude bands to the discussion in section 3.2. See more details in the reply to your specific comment below.

Furthermore, the results presented in Fig.7 and 8 which are the most important results of the paper suffer from the lack of analysis and discussions with previous studies. It is quite frustrating to read here “Analysis and attribution of the ozone changes over Eastern Asia is under investigation in a follow-up study”. Impact of drivers of tropospheric O₃ variations, of East Asian monsoon,... could be discussed and numerous previous studies should be cited. The focus of this paper is the demonstration of the creation of a joint TES and IASI data record. We have taken care to combine the data records from the two instruments in a way such that the combined record is meaningful. The time series are indeed intriguing, but we hope that the reviewer will appreciate that an in-depth analysis of the ozone record is beyond the scope of this paper.

In order to address the reviewer’s comment, we have removed the sentence beginning *Analysis and attribution...* and have added the following text to the end of that same paragraph:

For any given region, long-term variations in free tropospheric ozone can be affected by changes in local emissions of ozone precursors, changes in long-range transport within the troposphere and downward transport from the stratosphere (see e.g. Lin et al., 2012, 2014). The combined TES/IASI time series presented here has the potential to be used to aid attribution of the relative contributions from these effects, although such a study is outside the scope of this paper.

Specific comments:

p. 31031, l.5-8: It is not clear for me from panel b that the TES ozone profile shape deviates more from the a priori than the IASI one. I could even suspect the contrary.

Instead of showing TES and IASI profiles for all global surveys which mask the differences, would it be more appropriate to show one example for one individual survey or for one of the selected regions of interest (e.g. eastern Asia)?

While the mean TES profile values are closer to the mean prior values, the mean TES profile shows a steeper s-shape than IASI or the a priori.

Following suggestions of reviewer 2 and to emphasise the point we are trying to bring across we added to the discussion of Fig. 1 the following text:

Despite the fact that the ozone profiles themselves vary significantly with latitude and season owing to variations in tropopause altitude (Fig. 1B), the differences between IASI and TES ozone (Fig. 1D) are relatively consistent in shape and magnitude across seasons and latitudes, with the IASI-TES differences showing a standard deviation of only ~20 % in the upper troposphere for the whole dataset, compared to the extremely large standard deviations in the ozone upper tropospheric volume mixing ratio.

We also added the August and the November global survey example overviews to the supplementary material:

Two examples for the individual GS overviews are given in the supplementary material in Fig. S1 and Fig. S2 for August and November, respectively.

p. 31031, l. 22-23: Could you here mention the DOFS you obtain for the TES and IASI retrievals in that altitude range?

We moved the sentence: The degrees of freedom for signal for both TES and IASI for the considered altitude range are between 0.7 and 0.8. from p. 31034, l. 11-12 to p. 31031, l. 22-23.

p. 31031, l.26-27: This is not clear to me. Do you mean here the sum of the “rows” of averaging kernel matrix in the relevant pressure range: : :? But then how do you obtain one single value (x axis in figure 2) and not a sensitivity profile with 5 levels corresponding to the 5 retrieval vertical grid points in the selected pressure range? I do not understand what represents the “IASI sum of AK matrix” values you plot in fig.2. Please clarify.

We extended the text to read as follows:

The sum of the averaging kernel matrix in the relevant pressure range is used as a measure of the sensitivity. For this we calculate the sum of the rows of the AK matrix for each of the retrieval levels in the specified range and then add those together. The peak values of the TES AKs are larger than IASI's; however, the FWHM of the TES AK is narrower. Since we are averaging ozone over a range of several retrieval levels, the total area under the AKs is more representative of the information content than just the sum of the peak values.

p. 31032, l. 3-4: Figures 2 is quite hard to visualize and looking at that figure, it even seems that the IASI-TES differences are dependent on the ozone values with larger differences corresponding to large amount, while I agree that the differences seem independent on what you called here the IASI sensitivity.

We acknowledge that the choice of size-dependant markers was not ideal since it draws the eye to the outliers. We changed the figure to have the ozone amount marked with different colours instead.

p.31032, l.8: Some words of caution related to the impact of using different external parameters for TES and IASI retrievals on the IASI-TES differences should be added here.

We added to the text: Apart from instrument specifications, the sensitivity of infrared instruments towards ozone depends on the atmospheric and surface temperatures, water

vapour amount, residual cloud contamination, surface emissivity, and the amount of ozone itself. The uncertainties in the IASI ozone profile from the water vapour uncertainty has been estimated to be less than 2 % and from the temperature profile to be less than 5 % (Oetjen et al., 2014). The uncertainty from the surface temperature is negligible. Collocated retrievals, as considered here, should all be affected in a similar way by these external parameters.

p.31032, l.11-12: Do you obtain the same offset (3.9 ppb) when looking at different regions or at different time periods? What is the offset for the measurements over the three regions of interest? I would suggest to show the frequency distribution for the regions of interest in addition to the one you present for the global surveys, to get a feeling of the impact of the differences on the homogenized time series.

We did look at different latitude bands and seasons in the global survey dataset and we added a table with the parameters for the frequency distributions for those to the revised manuscript. Overall, we greatly expanded the discussion in section 3.2 for Fig. 3:

The normalised frequency distribution of the offset of the data of Fig. 2 is shown in Fig. 3. The distribution of the difference between TES and IASI-TOE follows roughly a Gaussian function with the maximum at (-3.9 ± 0.1) ppb (see Tab. 1, last row). For merging the TES and IASI-TOE data series, only the location of the peak value is important. The width of the frequency distribution is 17.6 ppb and is determined by the precision of the measurements and the collocation error: The precision for the IASI-TOE retrieval was estimated to be better than 20 % (see Sect 3.1). Those 20 % were calculated from comparison with ozone sondes with a coincidence criterion of also 55km (Oetjen et al., 2014). Hence a possible spatial collocation error is included in this estimate. This translates into 10.4 ppb for a mean IASI-TOE ozone of 51.9 ppb for the IASI precision plus spatial collocation. The TES precision of 15 % translates to 8.3 ppb for 55.4 ppb mean ozone. To estimate the temporal collocation error we compared model fields (GEOS-Chem version 10.1 (Bey et al., 2001; Eastham et al., 2014)) for the dates of the 4 global surveys for the overpass times of IASI and TES and calculated the standard deviation of the ozone difference which is 1.7 ppb. Adding the IASI combined precision and spatial collocation estimate, the TES precision and the temporal collocation estimate in quadrature gives ~14 ppb, which is slightly smaller than, but not dramatically different from the FWHM in Fig. 3.

Table 1 gives an overview for the Gaussian fit parameters for frequency distributions of selected sub-sets of the GSs separated by season or by latitude regions. Included are the location of the maxima and the FWHM of the Gaussian fit as well as the correlation coefficient R^2 for the quality of the fit to the data. In general the results are variable because of the large differences in sample size. However, when only considering distributions with an

R² larger than 0.95 (sub-samples for summer, winter, northern midlatitudes, and tropics), the peak values fall in the range of -3.4 to -4.9 ppb. This gives confidence in using a global offset of -3.9 ppb to combine TES and IASI average ozone mixing ratios in the chosen pressure range.

For the time series in the three regions of interests, we did not attempt to co-locate TES and IASI points (for the reasons discussed in the text). Therefore we do not have the frequency distribution for the ROIs.

p. 31034, l.15-16: Is the offset value of 3.9 ppb which has been determined for some specific short period at a global scale suitable for the three regions of interest?

This was determined using one global survey for each season over the course of 12 months, so the number is more representative than it would be for a single specific short period.

p. 31034, l. 21: Did you use a cloud fraction of 13% or 6% as previously mentioned in p. 1030, l.20?

We changed the sentence on p. 31034 to:

In this part of the study, we relax the cloud screening thresholds to 2.0 for the TES average cloud optical depth and to 13 % cloud fraction for IASI scenes which are more widely used thresholds (e.g. Clerbaux et al. 2009).

Technical corrections:

p.31032, l.16: I guess you mean “IASI-TES” differences, not IASI-TOE.

IASI-TOE: IASI - TES Optimal Estimation (see p. 31030, l. 2-3)

p.31033, l.26: “area the size” ! “area of the size”, same in the figure 5 caption.

Changed.

Reply to referee #2

We would like to thank the reviewer for his/her comments. The original review is shown below in blue with our comments in green.

This is a well-written and interesting paper looking at merging the data for tropospheric ozone from the TES and IASI instruments to provide a long-term time series. The selection of time series that have been derived show some interesting features, and such consistently merged time series will clearly be useful in studying tropospheric ozone trends. There are a few points of the paper that could have been discussed in more detail, and I think would benefit from further elaboration as detailed below:

Section 3.1, p.31030, lines 26-28: There is a statement that the 'average results did not change' with latitude or season. It would be useful to quantify this agreement or else show a plot showing evidence for this.

We acknowledge that the sentence is confusing in this context and we added instead more explanation further down in the paragraph when discussing specifically Fig 1D: *Despite the fact that the ozone profiles themselves vary significantly with latitude and season owing to variations in tropopause altitude (Fig 1B), the differences between IASI and TES ozone (Fig 1D) are relatively consistent in shape and magnitude across seasons and latitudes, with the IASI-TES differences showing a standard deviation of only ~20 % in the upper troposphere for the whole dataset, compared to the extremely large standard deviations in the ozone upper tropospheric volume mixing ratio.*

Section 3.2 and Figure 2:

a) This mentions in separate places that the differences between IASI and TES seem independent of the actual ozone amount, and a little later that very large differences coincide with large IASI ozone values, which seems contradictory. The figure is rather crowded, so it is hard to see if there is a dependence on ozone – it would be good to see this shown in a different way too for clarity.

We can appreciate that the discussion of Fig. 2, as worded, could appear contradictory. It is not that easy to separate the effects since the sensitivity of a measurement increases with the amount of ozone present. Hence we chose to combine the 3 parameters in one figure. However, using the size of the markers to represent the IASI ozone amount was an unfortunate choice since this draws the eye to the outliers. We changed the figure to have the ozone amount in colour-coded, same-size markers. We also removed that specific contradictory sentence to avoid confusion.

b) p.31032, line 14-16. It's stated that the width of the frequency distribution is determined by the precision of the measurements and the collocation error. Have you looked at whether this matches what you would expect theoretically?

The FWHM in Fig 3 is 17.6 ppb. The precision for the IASI-TOE retrieval was estimated to be better than 20%. Those 20% were calculated from comparison with ozone sondes with a coincidence criterion of also 55 km (Oetjen et al., 2014). Hence a possible spatial collocation error is included in this estimate. This translates into 10.4 ppb for a mean IASI-TOE ozone of 51.9 ppb for the IASI precision plus spatial collocation. The TES precision of 15% translates to 8.3 ppb for 55.4 ppb mean ozone. To estimate the temporal collocation error we compared model fields (GEOS-Chem, version 10.1 [Bey et al., 2001; Eastham et al., 2014]) for the dates of the 4 global surveys for the overpass times of IASI and TES and calculated the standard deviation of the ozone difference which is 1.7 ppb. Adding the IASI combined precision and spatial collocation estimate, the TES precision and the temporal collocation estimate in quadrature gives ~14 ppb, which is slightly smaller than, but not dramatically different from the FWHM in Fig 3. We added this to the text.

c) p.31032, Line 16-17: Are the outlying points all associated with realistic ozone retrievals, or could they also be symptoms of a problem with those retrieval points (e.g. cloud contamination?)

As the reviewer suggested in a) we removed this specific sentence from the manuscript (s.a.). However, the high values are all within the range of what one would expect from stratospheric intrusions or biomass burning plumes. The cloud filter with a cloud fraction of 6% or less for IASI retrievals is already very strict.

Section 4: The discontinuity in South East Asia is potentially very interesting. Have you investigated whether this is definitely a real affect in tropospheric ozone or if there could be any other possible reasons for this, e.g. instrumental factors, differences in inputs to the algorithm? Is this change seen in any of the input datasets for IASI? It is unfortunate that this seems to coincide exactly with the end of TES - are there any other data sources this could be validated against? You mentioned that there will be a more detailed paper on this, but it would still be useful to discuss here how confident you are that this is a real effect.

We added a figure to the manuscript showing a similar drop in ozone over Hilo, Hawaii. For that we averaged ozone sonde data over the same pressure range as TES and IASI (we did not apply the averaging kernels to the data).

Minor points:

Section 2, p31029: Line 16: 'For TES we use the publically available v05 level 2 Lite data'. Please clarify if this is the ozone dataset you are using, or just what you are using as input to the algorithm – it's a bit ambiguous at the moment.

The TES ozone results shown here are from the v05 Level 2 Lite data. We have updated the text to clarify.

Section 3.3, p 31034, line 2: 'We are aiming to sample' – this is in the future tense, whereas everything else talks about what has been done?

We changed this to present tense.

Technical corrections:

Section 1, p31027, line 6: 'De Smedt et al, 2009' – in the references there is given as 2010.

Corrected

Section 1, p31028, line 10: Metop was launched in 2006, not 2007 as stated.

Corrected

Overview of main changes:

- We added an ozone time series from sonde data over Hilo, Hawaii to show the similarities between Asian and remote Pacific ozone evolution.
- We changed the design of figure 2 since the previous version did not bring our point across that the difference of TES and IASI ozone is independent of the ozone amount.
- We added a quantitative discussion about the collocation error between TES and IASI ozone to show that we can explain the remaining variability. For this we looked at model ozone fields at the different overpass times.
- We added 2 figures to the supplementary information of the paper to show that the differences between TES and IASI are very similar for the individual global surveys and hence data from individual global surveys can be analysed in bulk.
- We added more explanations in several sections in the revised manuscript.

A Joint data record of tropospheric ozone from Aura-TES and MetOp-IASI

H. Oetjen^{1,2}, V. H. Payne¹, J. L. Neu¹, S. S. Kulawik^{1,3}, D. P. Edwards⁴, A. Eldering^{1,2}, H. M. Worden⁴, and J. R. Worden¹

[1]{Jet Propulsion Laboratory, California Institute of Technology, Pasadena, California}

[2]{The UCLA/JPL Joint Institute for Regional Earth System Science and Engineering, Los Angeles, California}

[3]{BAER Institute, Mountain View, California}

[4]{National Center for Atmospheric Research, Boulder, Colorado}

Correspondence to: V. H. Payne (Vivienne.H.Payne@jpl.nasa.gov)

Abstract

The Tropospheric Emission Spectrometer (TES) on Aura and Infrared Atmospheric Sounding Interferometer (IASI) on MetOp-A together provide a time series of ten years of free-tropospheric ozone with an overlap of three years. We characterise the differences between TES and IASI ozone measurements and find that IASI's coarser vertical sensitivity leads to a small (<5 ppb) low bias relative to TES for the free troposphere. The TES-IASI differences are not dependent on season or any other factor and hence the measurements from the two instruments can be merged, after correcting for the offset, in order to study decadal-scale changes in tropospheric ozone. We calculate time series of regional monthly mean ozone in the free troposphere over Eastern Asia, the Western United States (US), and Europe, carefully accounting for differences in spatial sampling between the instruments. We show that free-tropospheric ozone over Europe and the Western US has remained relatively constant over the past decade, but that, contrary to expectations, ozone over Asia in recent years does not continue the rapid rate of increase observed from 2004–2010.

1 **1 Introduction**

2 Tropospheric ozone adversely impacts human health and ecosystems at the Earth's surface,
3 and plays a key role in photochemistry throughout the troposphere. Ozone also acts as a
4 greenhouse gas in the upper troposphere (e.g. Gauss et al., 2003; Worden et al., 2008,
5 Bowman and Henze, 2012). Sources of tropospheric ozone include photo-chemical
6 production from non-methane volatile organic compounds (NMVOCs) and carbon monoxide
7 (CO) in the presence of nitrogen oxide radicals (NO_x) as well as transport from the
8 stratosphere into the troposphere (e.g. Worden et al., 2009; Young et al., 2013; Neu et al.,
9 2014).

10 The lifetime of ozone in the free troposphere is on the order of several weeks (e.g. Stevenson
11 et al., 2006). Hence regional changes in ozone precursor emissions or in transport can have
12 implications for tropospheric ozone concentrations on a global scale. In recent years, rapid
13 urbanisation and industrialisation in China have led to large changes in ozone precursor
14 emissions. Measurements over Asia have shown ozone increasing in the decade leading up to
15 2010 (e.g. Tanimoto et al., 2009; Wang et al., 2012; Lee et al., 2014). Increases in NO_x (for
16 NO_2 see e.g. van der A et al., 2008; Hilboll et al., 2013) and NMVOCs (for formaldehyde see
17 De Smedt et al., 2009) - as well as tropospheric ozone (Beig and Singh, 2007) - have been
18 observed from space, although CO has been shown to be decreasing over China (Worden et
19 al., 2013).

20 Emissions from China dominate the Asian pollutant outflow (e.g. Zhang et al, 2009). Several
21 studies report trans-Pacific transport of pollution plumes (e.g. Zhang et al., 2008; Singh et al.,
22 2009). With increasing Asian pollution, an enhancement of ozone concentrations in the
23 Western US is expected (Jiang et al., 2015). Several model studies (e.g. Jacob et al., 1999;
24 Wild and Akimoto, 2001; Fiore et al., 2009; Reidmiller et al., 2009; Lin et al., 2012; Fry et
25 al., 2013; 2014) evaluated the intercontinental impact of ozone precursors emissions in mid-
26 latitude industrial areas on the ozone concentrations in downwind regions. Increases in Asian
27 pollution have previously been assumed to be associated with positive trends in ozone in the
28 Western US (Jaffe and Ray, 2007; Parrish et al., 2009; Cooper et al., 2010; Verstraeten et al.,
29 2015).

30 Pollutant trends for Europe and Northern America do not provide such a consistent picture.
31 Ebojie et al. (2015) have found negative albeit not significant trends of tropospheric ozone
32 columns over the Western US analysing SCIAMACHY measurements for the period of 2003

1 to 2011. On the other hand, parts of Europe show a significant negative trend in the
2 SCIAMACHY data (Ebojie et al., 2015). Cooper et al. (2014) compiled ground-based surface
3 ozone measurements and lowermost tropospheric measurements from aircraft and ozone
4 sondes and calculated trends beginning 1990–1999 through 2000–2010 and found mostly
5 positive trends for the Western US and negative ones for the Eastern US. Europe showed a
6 positive ozone trend in this data set. However as pointed out by Cooper et al. (2014),
7 European ground-based measurements do not show a positive trend from about 2000
8 onwards. NO₂ tropospheric columns have been reported to decrease over North America and
9 Europe (e.g. Hillboll et al., 2013).

10 The Tropospheric Emission Spectrometer (TES), launched on-board the Aura satellite in
11 2004, was specifically designed to measure tropospheric ozone by means of fine spectral
12 resolution (0.1 cm⁻¹) radiance measurements in the thermal infrared. However, the near-global
13 TES record of tropospheric ozone ended in 2011 when the TES observing strategy shifted
14 away from routine *global survey* measurements in order to focus on special observations over
15 select regions, to preserve the lifetime of the instrument. The Infrared Atmospheric Sounding
16 Instruments (IASI), flying on the MetOp satellites since the launch of MetOp-A in 2007 and
17 continuing with Metop-B in 2012, are designed for both atmospheric composition and
18 numerical weather prediction applications (Clerboux et al. 2009). Although the spectral
19 resolution of the IASI measurements, at 0.5 cm⁻¹, is coarser than TES, IASI retrievals have
20 been shown to provide a wealth of useful information on tropospheric ozone (e.g. Dufour et
21 al, 2010; Safieddine et al, 2013; Oetjen et al., 2014). The IASI instruments offer the dual
22 advantages of extensive spatial coverage and a record that is assured to continue well into the
23 future with the launch of the Metop-C platform in 2018. Here we show that TES and IASI
24 ozone measurements can be combined and used to investigate changes in tropospheric ozone
25 over the past decade, with a focus on Eastern Asia, the Western US and Europe.

26

27 **2 Satellite measurements of tropospheric ozone from TES and IASI:** 28 **Observations and retrieval approach**

29 IASI-1 flies in a sun-synchronous orbit on MetOp-A. The local overpass times at the equator
30 are 9:30 and 21:30. IASI is a scanning instrument and achieves global coverage twice daily.
31 At nadir, the footprint is a circle with 12 km diameter, while on the sides of the swath the
32 footprint is elongated elliptically to 20 km × 39 km. TES on the AURA satellite, on the other

1 hand, measures in the nadir only, with a rectangular surface footprint of 5.3 km × 8.3 km.
2 TES orbits are separated by 22° longitude and in the nominal observation mode (which is
3 used in this study, and called *global survey*), measurements are taken every 182 km along the
4 flight track. The equator crossing times are 1:45 and 13:45. TES has a spectral resolution of
5 0.1 cm⁻¹ full-width half-maximum (FWHM) and a spectral sampling of 0.06 cm⁻¹. IASI
6 measures with a coarser resolution of 0.5 cm⁻¹ FWHM and a sampling of 0.25 cm⁻¹, resulting
7 in slightly less vertical information for the trace gas retrievals (Oetjen et al., 2014). The noise
8 equivalent differential temperatures are 0.15 K at 280 K and 0.3 K at 300 K for IASI and
9 TES, respectively. In this work, the TES optimal estimation retrieval algorithm (Bowman et
10 al., 2002; 2006) has been applied to the IASI radiances in order to maintain consistency
11 between the records in terms of a priori constraints and retrieval method. One difference we
12 maintain is that for TES, temperature, clouds, and emissivity, all important parameters for an
13 accurate ozone retrieval, are also retrieved with the TES algorithm in steps before the actual
14 ozone analysis. For IASI, we use the operational EUMETSAT level 2 data for temperature
15 and clouds and we use the Zhou climatology for emissivity (Zhou et al., 2011). [The TES](#)
16 [ozone results shown here are from the v05 Level 2 Lite data.](#) ~~For TES, we use the publicly~~
17 ~~available V05 level 2 Lite data~~ (<http://tes.jpl.nasa.gov/data/>). Details for the retrievals can be
18 found in (Bowman et al., 2006; Kulawik et al., 2006; Oetjen et al., 2014).

19

20 **3 Construction of a combined ozone record**

21 Combining TES and IASI measurements into a merged time series requires careful
22 consideration of differences in sensitivity and sampling. No differences due to the retrieval
23 settings are expected since the same algorithm, a priori profiles and constraints have been
24 applied to the radiances of the two instruments. In this section, we describe the methodology
25 for comparing and homogenising the datasets.

26 **3.1 Characterisation of retrieval profile differences**

27 Estimates of tropospheric ozone based on IASI radiances and the TES optimal estimation
28 algorithm (IASI-TOE) have been validated against sonde data in previous work; details of the
29 prior constraints, retrieval levels and spectral windows, as well as the predicted and actual
30 errors and the biases with respect to the sondes, can be found in Oetjen et al. (2014). Biases of
31 TES ozone with respect to ozonesondes are investigated in Verstraeten et al. (2013). Both

1 instruments show a similar positive bias in the upper troposphere/ lower stratosphere in
2 comparison to sondes. This bias is believed to originate from incorrect spectroscopic
3 parameters (e.g. Oetjen et al., 2014). Here, we quantify differences between TES and IASI-
4 TOE ozone in order to assess the feasibility of merging the time series of the two instruments.
5 We select four TES global surveys (GSs) approximately three months apart (3–4 August
6 2008, 1–2 November 2008, 17–18 February 2009, 26–27 May 2009; a GS takes about 26 hr
7 and these were chosen since they had the highest number of successful retrievals in the
8 corresponding months) and compare the ozone profiles and retrieval sensitivities with co-
9 located IASI-TOE retrievals. The coincidence criteria are 55 km (corresponding to 0.5°
10 latitude) and 5 hr. The time difference, which is larger than typically used for defining
11 coincident trace gas profiles, is driven by the different overpass times of the Aura and MetOp-
12 A satellites. TES scenes with an average cloud optical depth of 0.1 or less and IASI scenes
13 with a cloud fraction of 6 % or less are included. Further for TES, the data were filtered by
14 the retrieval quality and the C-curve flags (see TES user guides,
15 <http://tes.jpl.nasa.gov/documents/>) and IASI was limited to retrievals with a χ^2 less than 1.3
16 (see Oetjen et al., 2014). Because of IASI's dense sampling, there can be multiple IASI co-
17 locations for a TES scene. Overall, there are 3992 IASI measurements and 745 TES
18 measurements for the four TES global surveys. Results of the TES-IASI comparison are
19 shown in Fig. 1 for all GSs together. ~~The average results did not change when looking at the~~
20 ~~individual GSs, at different latitude band, or at seasonal differences.~~ Panels A and B show the
21 average profile of the sum of the rows of the averaging kernel (AK) matrices and of ozone
22 along with their standard deviations, respectively. The TES sensitivity is slightly better than
23 IASI throughout most of the atmosphere as expected due to the finer spectral resolution of
24 TES compared to IASI. The differences in the sensitivity are likely the reason for the different
25 ozone profile shapes for TES and IASI-TOE; while the mean IASI-TOE ozone follows the
26 general shape of the a priori profile (although not its absolute values), the mean TES profile
27 shape deviates from the a priori profile shape in the mid- and upper-troposphere. The large
28 standard deviation on the ozone profile in the stratosphere results from the rather large
29 latitudinal range that is covered by the measurements: 50°S–80°N. This also includes some
30 profiles affected by the ozone hole at high latitude. The relative differences are shown in
31 panels C and D, plotted as the mean of the individual differences. On average, IASI ozone
32 abundances are less than those from TES between the surface and ~250 hPa, with a maximum
33 difference of -13 % at 500 hPa. Above 250 hPa, IASI-TOE ozone is greater than TES ozone,

1 with a maximum difference of 8 % at about 150 hPa. Despite the fact that the ozone profiles
2 themselves vary significantly with latitude and season owing to variations in tropopause
3 altitude (Fig. 1B), the differences between IASI and TES ozone (Fig. 1D) are relatively
4 consistent in shape and magnitude across seasons and latitudes, with the IASI-TES
5 differences showing a standard deviation of only ~20 % in the upper troposphere for the
6 whole dataset, compared to the extremely large standard deviations in the ozone upper
7 tropospheric volume mixing ratio. Note that the differences between IASI-TOE and TES
8 approach zero at the surface and towards the top at the atmosphere because the retrievals
9 essentially return the a priori in these regions due to the low sensitivities. The IASI-TOE
10 precision in the free troposphere was estimated to be better than 20 % (Oetjen et al., 2014).
11 TES precision in the free troposphere has previously been shown to be 10-15% (Boxe et al.,
12 2010). Therefore TES and IASI-TOE ozone profiles agree well within their respective
13 uncertainties. Two examples for the individual GS overviews are given in the supplementary
14 material in Fig. S1 and Fig. S2 for August and November, respectively.

15 **3.2 Characterisation of differences for column-averaged mixing ratios**

16 In the following, we present results on column-average mixing ratios between 681 and
17 316 hPa, a range where both the TES and IASI-TOE ozone retrievals show good sensitivity.
18 The degrees of freedom for signal for both TES and IASI for the considered altitude range are
19 between 0.7 and 0.8. This range includes 5 retrieval vertical grid points and the data is the
20 same collocated data as in Sect. 3.1.

21 The differences between TES and IASI partial column mean mixing ratios as a function of the
22 IASI-TOE sensitivity is shown in Fig. 2. The sum of the averaging kernelAK matrix in the
23 relevant pressure range is used as a measure of the sensitivity. For this we calculate the sum
24 of the rows of the AK matrix for each of the retrieval levels in the specified range and then
25 add those together. The peak values of the TES AKs are larger than IASI's; however, the
26 FWHM of the TES AKs is narrower. Since we are averaging ozone over a range of several
27 retrieval levels, the total area under the AKs is more representative of the information content
28 than just the sum of the peak values. The diameter of the symbols is proportional to the mean
29 IASI-TOE ozone mixing ratio. The data points in fig. 2 are colour-coded for the mean IASI-
30 TOE ozone mixing ratio as indicated in the legend. Although the sensitivity of the ozone
31 retrievals depends on the amount of ozone itself and although there is a wide range of the
32 (IASI – TES) differences, these differences appear to be independent of the sensitivity and the

1 actual ozone amount (see Fig. 2). Apart from instrument specifications, the sensitivity of
2 infrared instruments towards ozone depends on the atmospheric and surface temperatures,
3 water vapour amount, residual cloud contamination, surface emissivity, and the amount of
4 ozone itself. [The uncertainties in the IASI ozone profile from the water vapour uncertainty](#)
5 [has been estimated to be less than 2 % and from the temperature profile to be less than 5 %](#)
6 [\(Oetjen et al., 2014\). The uncertainty from the surface temperature is negligible.](#) Collocated
7 retrievals [as considered here,](#) should all be affected in a similar way by these external
8 parameters. However, the instrumental difference in the spectral resolution of TES and IASI
9 results in different weighting functions that gives a simple offset between the ozone retrievals.

10 The normalised frequency distribution of the offset of the data of Fig. 2 is shown in Fig. 3.
11 The distribution of the difference between TES and IASI-TOE follows roughly a Gaussian
12 function with the maximum at (-3.9 ± 0.2) ppb [\(see Tab. 1, last row\)](#). For merging the TES
13 and IASI-TOE data series, only the location of the peak value is important. The width of the
14 frequency distribution is [17.6 ppb and is](#) determined by the precision of the measurements and
15 the collocation error: [The precision for the IASI-TOE retrieval was estimated to be better than](#)
16 [20 % \(see Sect 3.1\). Those 20 % were calculated from comparison with ozone sondes with a](#)
17 [coincidence criterion of also 55km \(Oetjen et al., 2014\). Hence a possible spatial collocation](#)
18 [error is included in this estimate. This translates into 10.4 ppb for a mean IASI-TOE ozone of](#)
19 [51.9 ppb for the IASI precision plus spatial collocation. The TES precision of 15 % translates](#)
20 [to 8.3 ppb for 55.4 ppb mean ozone. To estimate the temporal collocation error we compared](#)
21 [model fields \(GEOS-Chem version 10.1 \(Bey et al., 2001; Eastham et al., 2014\)\) for the dates](#)
22 [of the 4 global surveys for the overpass times of IASI and TES and calculated the standard](#)
23 [deviation of the ozone difference which is 1.7 ppb. Adding the IASI combined precision and](#)
24 [spatial collocation estimate, the TES precision and the temporal collocation estimate in](#)
25 [quadrature gives ~14 ppb, which is slightly smaller than, but not dramatically different from](#)
26 [the FWHM in Fig. 3-](#)

27 [Table 1 gives an overview for the Gaussian fit parameters for frequency distributions of](#)
28 [selected sub-sets of the GSs separated by season or by latitude regions. Included are the](#)
29 [location of the maxima and the FWHM of the Gaussian fit as well as the correlation](#)
30 [coefficient \$R^2\$ for the quality of the fit to the data. In general the results are variable because](#)
31 [of the large differences in sample size. However, when only considering distributions with an](#)
32 [\$R^2\$ larger than 0.95 \(sub-samples for summer, winter, northern midlatitudes, and tropics\), the](#)

1 peak values fall in the range of -3.4 to -4.9 ppb. This gives confidence in using a global offset
2 of -3.9 ppb to combine TES and IASI average ozone mixing ratios in the chosen pressure
3 range.

4 ~~The points with very large IASI TOE differences are generally associated with large IASI-~~
5 ~~TOE ozone values. Most likely, this is symptomatic of the loose temporal coincidence~~
6 ~~criterion. Atmospheric phenomena that cause very high ozone in the free troposphere (e.g.~~
7 ~~biomass burning or stratospheric intrusions) often occur on time scales shorter than 5 hr.~~

8 **3.3 Sampling considerations**

9 Between 2004 and 2011, the nominal mode of TES operation involved GSs with regular
10 sampling over the globe. In 2011, the TES observing strategy shifted away from routine GS
11 measurements in order to focus on special observations over select regions, to preserve the
12 lifetime of the instrument. IASI-1, on MetOp-A, has been operational since 2007. IASI-2, on
13 MetOp-B, was launched in 2012. The IASI series will be continued with future missions, with
14 IASI-3 on MetOp-C planned for 2017/18 and three IASI-NG (next generation) missions
15 planned after that.

16 IASI data is not currently routinely processed through the TES algorithm, which was
17 originally set up for relatively small TES-like, rather than IASI-like, data volumes.
18 Therefore, for this work we choose to process a subset of IASI scenes over selected regions of
19 interest (ROIs – shown in Fig. 4) for the construction of the combined time series. We
20 evaluate the consistency of the TES and IASI-1 monthly mean column-average mixing ratios
21 for these ROIs, using the overlap between datasets in the years 2008-2011.

22 Compared to IASI, the TES sampling is sparse. One approach to constructing the time series
23 would be to restrict the data to collocated TES and IASI points, for cases where both are
24 deemed to be sufficiently clear-sky. However, we find that this approach leads to an
25 unacceptable reduction in the number of TES data points (see below). Therefore, we instead
26 choose to sub-sample the IASI data over the ROIs without the requirement of co-location with
27 TES points. The impact of the IASI sub-sampling is explored below.

28 IASI scenes with sample sizes ranging from 50 to 2000 were randomly selected within the
29 Eastern Asia ROI for May 2009. The resulting monthly mean ozone is presented in Fig. 5.
30 The error bars are the 95 % confidence limits CL for the mean x_{mean} , assuming a normal
31 distribution calculated from:

$$1 \quad CL = x_{mean} \pm 1.96 \frac{\sigma}{\sqrt{N}} \quad (1)$$

2 with σ being the sample standard deviation and N the sample size. These confidence limits for
3 the monthly mean are an approximation since ozone itself is neither temporally nor spatially
4 uncorrelated in the atmosphere. The actual sample standard deviation [of about 15 ppb](#) ~~(not~~
5 ~~shown)~~ does not change with the sample size [\(not shown\)](#) and hence the confidence limits
6 vary with the square-root of the sample size only. This indicates that it is valid to assume a
7 normal distribution for the ozone, at least for the given example. We conclude that a sample
8 of 200 IASI scenes is sufficient for an uncertainty of 1.9 ppb or better for an area [of](#) the size
9 of the Eastern Asia box. This is about 2–3 % of the mean mixing ratio for the chosen ROIs
10 and about 10 % of the variation observed for the deseasonalised time series (see Sect. 4). The
11 areas of the Western US and Europe ROIs scale by a factor of 1.28 and 1.20, respectively, and
12 ~~we are aiming~~ to sample at least 250 scenes for those ROIs. In many cases, larger sample
13 sizes have been used. This is due to the fact that a larger number than the number of target
14 scenes is selected first and then the actual throughput of successfully retrieved ozone profiles
15 depends on the quality screening (see Fig. S43 in the Supplement for the sample sizes). On
16 average for all the years in the time series below, the IASI limits of confidence are 1.9 ppb,
17 1.7 ppb, and 1.5 ppb for the Eastern Asia, Western US, and Europe ROI, respectively. In the
18 example shown in Fig. 5, the TES confidence limit is 2.3 ppb for 128 scenes. In general, there
19 are less TES scenes than IASI scenes and the average confidence limit for all ROIs for TES
20 monthly mean ozone is 2.6 ppb. ~~The degrees of freedom for signal for both TES and IASI for~~
21 ~~the considered altitude range are between 0.7 and 0.8.~~ An example for the spatial distribution
22 of the satellite scenes is presented in Fig. 6 for 206 IASI data points.

23

24 **4 Results**

25 Figure 7 shows the time series of partial column ozone for the 3 ROIs. In these figures, the
26 IASI monthly means have been adjusted by a constant value of +3.9 ppb based on our
27 analysis in Sect. 3.2. There is an overlap of about 3 years between TES and IASI for Eastern
28 Asia and the Western US ROIs. Over Europe, the overlap is only ~2 years because the
29 latitude range of the TES GSs was limited to 30°S–50°N from 2010 onward. [Here](#)[In this part](#)
30 [of the study, we relax](#) the cloud screening thresholds ~~are to~~ 2.0 for the TES average cloud

1 optical depth and to 13 % cloud fraction for IASI scenes which are more widely used
2 thresholds (e.g. Clerbaux et al. 2009)-

3 ~~Data gaps in the time series occur for several reasons. Data has been removed if an instrument~~
4 ~~has missing data for more than a week of any given month or if the ROI is not completely~~
5 ~~sampled spatially by an instrument. Also, since the IASI data is chosen with a random number~~
6 ~~generator from all of the available scenes, if the initial distribution of scenes is already biased~~
7 ~~and not random due to some missing orbits caused by instrumental problems, then a specific~~
8 ~~time or location can be oversampled relative to the rest of the month or region. This data is~~
9 ~~removed as well.~~ Data gaps in the time series occur for several reasons. A data point for a
10 whole month is removed if an instrument has missing data for more than a week for that given
11 month or if the whole area of the ROI is not completely covered by an instrument due to
12 cloud cover or missing orbits. Missing orbits can lead to biased sampling of the random
13 number generator within the ROI of a given month. However, the data has been screened for
14 this by looking at the number of satellite scenes per day used for calculating the monthly
15 mean: If the number of satellite scenes for 3 or more consecutive days is twice as high as the
16 average for the rest of the month, the monthly data points are removed as well. For all data
17 points included in the time series, care was taken to ensure that the initial distribution is
18 unbiased.

19 TES and IASI agree well for the overlap period; differences are mostly within the range of
20 less than 4.5 ppb as expected from the calculated confidence limits (see Sect. 3.3). In
21 particular, Eastern Asia shows very good agreement between TES and IASI-TOE ozone for
22 2008–2011, giving confidence in the consistency of the time series. There are a few cases
23 where IASI ozone exceeds TES ozone by more than the confidence limits of the monthly
24 mean, e.g. February 2008 for Eastern Asia or January 2009 for the Western US ROI. These
25 instances can be traced back to some localised enhanced ozone which was not detected by
26 TES' coarser sampling and in these cases the required condition for randomness for using Eq.
27 1 is not fulfilled. The variation over the 10 years of data is dominated by the seasonal cycle.

28 Figure 8 shows the deseasonalised time series for the 3 ROIs, in order to better show the long-
29 term variations in ozone for the 2004–2014 time period. We remove the seasonal variation by
30 calculating the mean ozone over all of the years for each month and subtracting this mean
31 from the respective months in the time series. For the years where TES and IASI overlap, the
32 mean of the 2 data points is used. From November 2004 to May 2005, TES measured with a

1 somewhat sparser sampling pattern than the period after May 2005 and consequently the error
2 on the monthly mean is larger for this portion of the time series because there are fewer data
3 points to average (See Fig. S3). This data was excluded from the calculation of the overall
4 monthly mean used to deseasonalise the data.

5 As seen in Fig. 8, ozone over Eastern Asia rose relatively steadily from 2004–2010, but
6 dropped suddenly in 2011. This is also clearly apparent when looking only at the annual
7 maxima in Fig. 7. While ozone has been somewhat increasing once again since 2011, a clear
8 upward trend is not observed and ozone has also not yet reached pre-2011 values. [A similar
9 sharp drop in 2011 can also be observed in ozone sonde data over Hilo, Hawaii \(see Fig. 9\), a
10 location strongly influenced by outflow of free tropospheric air from Asia \(Lin et al., 2014\).
11 The ozone mixing ratios measured by the sondes between 681 and 316 hPa, the same pressure
12 range as for TES and IASI, have been averaged and then deseasonalised. We used the full
13 dataset since 1991 to remove the seasonality, but we only show the same years as for the
14 combined TES and IASI time series starting in 2004. Note that we have not applied the
15 satellite AKs to the sonde profiles and the ozone data in Fig. 9 is completely independent of
16 the TES and IASI measurements. ~~Analysis and attribution of the ozone changes over Eastern
17 Asia is under investigation in a follow-up study. For any given region, long-term variations in
18 free tropospheric ozone can be affected by changes in local emissions of ozone precursors,
19 changes in long-range transport within the troposphere and downward transport from the
20 stratosphere \(see e.g. Lin et al., 2012, 2014\). The combined TES/IASI time series presented
21 here have the potential to be used to aid attribution of the relative contributions from these
22 effects, although such a study is outside the scope of this paper.~~](#)

23 In contrast to Eastern Asia, ozone over the Western US and Europe has remained relatively
24 constant over the past decade. The time series for these regions are dominated by interannual
25 variability, some of which is coherent in all three regions (for example, high ozone in spring
26 2008 and high ozone in 2010 followed by lower ozone in 2011).

27 28 **5 Summary and discussion**

29 We have assessed the consistency between time series of tropospheric ozone from TES and
30 IASI-TOE retrievals, using a consistent retrieval algorithm applied to the radiances of both
31 instruments. TES exhibits slightly better sensitivity than IASI, due to the finer spectral
32 resolution of the TES instrument. Despite the small differences in sensitivity, the time series

1 of the 681–316 hPa partial column-averaged ozone mixing ratios show good agreement for
2 the years 2008–2011, after the removal of a constant -3.9 ppb offset from TES in the IASI-
3 TOE record.

4 Combined TES and IASI monthly-mean time series were constructed for three regions of
5 interest: Eastern Asia, the Western US and Europe. Ozone has remained relatively constant
6 over the Western US and Europe over the past decade, and ozone changes in those regions are
7 dominated by seasonal and interannual variability. The deseasonalised time series for Eastern
8 Asia, on the other hand, shows an overall increase between 2004 and 2010, with a drop in
9 2011 followed by a slow or no increase through 2014. Somewhat surprisingly, ozone over
10 Eastern Asia has not yet returned to pre-2011 levels. To the best of our knowledge, only one
11 study, by Chen et al. (2014), suggests that the rapid increase in ozone over Asia may have
12 levelled-off in recent years. That study, however, focused on Taiwan and found that a change
13 in the slope of the ozone trend from 1994–2012 occurred in 2007. The complex temporal
14 changes in ozone over Eastern Asia show that ozone changes driven by changing
15 concentrations of precursor gases and other sources, such as stratosphere-troposphere-
16 exchange, still need to be better-understood in the context of long-term trends and prognoses.
17 Understanding what drives changes in ozone over Eastern Asia is particularly critical for air
18 quality in the Western U. S., since it has been speculated that transport of increasing ozone
19 from Asia may contribute to non-attainment of EPA air quality standard in the future (e.g.
20 Hudman et al., 2004).

21

22 **Acknowledgements**

23 We acknowledge the NOAA/CLASS data centre for the IASI Level 1c spectra and
24 EUMETSAT for the Level 2 data. IASI is a joint mission of EUMETSAT and the Centre
25 National d'Études Spatiales (CNES, France). Part of the research was carried out at the Jet
26 Propulsion Laboratory, California Institute of Technology, under a contract with the National
27 Aeronautics and Space Administration. We acknowledge NASA support under the grant
28 NNX11AE19G. [The Hilo ozone sonde data were provided by the Global Monitoring Division
29 of NOAA \(www.esrl.noaa.gov/gmd\).](#)

30

31

1 **References**

- 2 Beig, G., and Singh, V.: Trends in tropical tropospheric column ozone from satellite data and
3 MOZART model, *Geophys. Res. Lett.*, 34, L17801, doi:10.1029/2007GL030460, 2007.
- 4 [Bey, I., Jacob D., J., Yantosca, R. M., Logan, J. A., Field, B., Fiore, A. M., Li, Q., Liu, H.,
5 Mickley, L. J., and Schultz, M.: Global modeling of tropospheric chemistry with assimilated
6 meteorology: Model description and evaluation, *J. Geophys. Res.*, 106, 23,073-23,096, 2001.](#)
- 7 Bowman, K. W., Worden, J., Steck, T., Worden, H. M., Clough, S., and Rodgers, C.:
8 Capturing time and vertical variability of tropospheric ozone: A study using TES nadir
9 retrievals, *J. Geophys. Res.*, 107, 4723, doi:10.1029/2002JD002150, 2002.
- 10 Bowman, K. W., Rodgers, C. D., Kulawik, S. S., Worden, J., Sarkissian, E., Osterman, G.,
11 Steck, T., Lou, M., Eldering, A., Shephard, M., Worden, H., Lampel, M., Clough, S., Brown,
12 P., Rinsland, C., Gunson, M., and Beer, R.: Tropospheric emission spectrometer: Retrieval
13 method and error analysis, *IEEE T. Geosci. Remote*, 44, 1297–1307,
14 doi:10.1109/tgrs.2006.871234, 2006.
- 15 Bowman, K., and Henze, D. K.: Attribution of direct ozone radiative forcing to spatially
16 resolved emissions, *Geophys. Res. Lett.*, 39(22), doi:10.1029/2012GL053274, 2012.
- 17 Boxe, C. S., Worden, J. R., Bowman, K. W., Kulawik, S. S., Neu, J. L., Ford, W. C.,
18 Osterman, G. B., Herman, R. L., Eldering, A., Tarasick, D. W., Thompson, A. M., Doughty,
19 D. C., Hoffmann, M. R., and Oltmans, S. J.: Validation of northern latitude Tropospheric
20 Emission Spectrometer stare ozone profiles with ARC-IONS sondes during ARCTAS:
21 sensitivity, bias and error analysis, *Atmos. Chem. Phys.*, 10(20), 9901–9914,
22 doi:10.5194/acp-10-9901-2010, 2010.
- 23 Chen, S.-P., Chang, C.-C., Liu, J.-J., Chou, C. C.-K., Chang, J. S., and Wang, J.-L.: Recent
24 improvement in air quality as evidenced by the island-wide monitoring network in Taiwan,
25 *Atmos. Environ.*, Volume 96, Pages 70-77, doi:10.1016/j.atmosenv.2014.06.060, 2014
- 26 Clerbaux, C., Boynard, A., Clarisse, L., George, M., Hadji-Lazaro, J., Herbin, H., Hurtmans,
27 D., Pommier, M., Razavi, A., Turquety, S., Wespes, C., and Coheur, P.-F.: Monitoring of
28 atmospheric composition using the thermal infrared IASI/MetOp sounder, *Atmos. Chem.
29 Phys.*, 9, 6041–6054, doi:10.5194/acp-9-6041-2009, 2009.

1 Cooper, O. R., Parrish, D. D., Stohl, A., Trainer, M., Nedelec, P., Thouret, V., Cammas, J. P.,
2 Oltmans, S. J., Johnson, B. J., Tarasick, D., Leblanc, T., McDermid, I. S., Jaffe, D., Gao, R.,
3 Stith, J., Ryerson, T., Aikin, K., Campos, T., Weinheimer, A., and Avery, M. A.: Increasing
4 springtime ozone mixing ratios in the free troposphere over western North America, *Nature*,
5 463(7279), 344–348, doi:10.1038/nature08708, 2010.

6 Cooper, O. R., Parrish, D. D., Ziemke, J., Balashov, N. V., Cupeiro, M., Galbally, I.E., Gilge,
7 S., Horowitz, L., Jensen, N.R., Lamarque, J.-F., Naik, V., Oltmans, S.J., Schwab, J., Shindell,
8 D.T., Thompson, A.M., Thouret, V., Wang, Y., and Zbinden, R.M.: Global distribution and
9 trends of tropospheric ozone: An observation-based review. *Elem. Sci. Anth.* 2: 000029 doi:
10 10.12952/journal.elementa.000029, 2014.

11 De Smedt, I., Stavrou, T., Müller, J.-F., van der A, R. J., and Van Roozendaal, M.: Trend
12 detection in satellite observations of formaldehyde tropospheric columns, *Geophys. Res.*
13 *Let.*, 37, L18808, doi:10.1029/2010GL044245, 2009.

14 Dufour, G., Eremenko, M., Orphal, J., and Flaud, J.-M.: IASI observations of seasonal and
15 day-to-day variations of tropospheric ozone over three highly populated areas of China:
16 Beijing, Shanghai, and Hong Kong, *Atmos. Chem. Phys.*, 10, 3787-3801, doi:10.5194/acp-10-
17 3787-2010, 2010.

18 [Eastham, S. D., Weisenstein, D. K., and Barrett, S. R. H.: Development and evaluation of the](#)
19 [unified tropospheric-stratospheric chemistry extension \(UCX\) for the global chemistry-](#)
20 [transport model GEOS-Chem, *Atmos. Env.*, 89, 52-63, 2014.](#)

21 Ebojio, F., Burrows, J. P., Gebhardt, C., Ladstätter-Weissenmayer, A., von Savigny, C.,
22 Rozanov, A., Weber, M., and Bovensmann, H.: Global and zonal tropospheric ozone
23 variations from 2003–2011 as seen by SCIAMACHY, *Atmos. Chem. Phys. Discuss.*, 15,
24 24085-24130, doi:10.5194/acpd-15-24085-2015, 2015.

25 Fiore, A. M., Dentener, F. J., Wild, O., Cuvelier, C., Schultz, M. G., Hess, P., Textor, C.,
26 Schulz, M., Doherty, R. M., Horowitz, L. W., MacKenzie, I. A., Sanderson, M. G., Shindell,
27 D. T., Stevenson, D. S., Szopa, S., van Dingenen, R., Zeng, G., Atherton, C., Bergmann, D.,
28 Bey, I., Carmichael, G., Collins, W. J., Duncan, B. N., Faluvegi, G., Folberth, G., Gauss, M.,
29 Gong, S., Hauglustaine, D., Holloway, T., Isaksen, I. S. A., Jacob, D. J., Jonson, J. E.,
30 Kaminski, J. W., Keating, T. J., Lupu, A., Marmer, E., Montanaro, V., Park, R. J., Pitari, G.,
31 Pringle, K. J., Pyle, J. A., Schroeder, S., Vivanco, M. G., Wind, P., Wojcik, G., Wu, S., and

1 Zuber, A.: Multimodel estimates of intercontinental source-receptor relationships for ozone
2 pollution, *J. Geophys. Res.*, 114(D4), D04301, doi:10.1029/2008JD010816, 2009.

3 Fry, M. M., Schwarzkopf, M. D., Adelman, Z., Naik, V., Collins, W. J., and West, J. J.: Net
4 radiative forcing and air quality responses to regional CO emission reductions, *Atmos. Chem.*
5 *Phys.*, 13, 5381-5399, doi:10.5194/acp-13-5381-2013, 2013.

6 Fry, M. M., Schwarzkopf, M. D., Adelman, Z., and West, J. J.: Air quality and radiative
7 forcing impacts of anthropogenic volatile organic compound emissions from ten world
8 regions, *Atmos. Chem. Phys.*, 14, 523-535, doi:10.5194/acp-14-523-2014, 2014.

9 Gauss, M., Myhre, G., Pitari, G., Prather, M. J., Isaksen, I. S. A., Berntsen, T. K., Brasseur, G.
10 P., Dentener, F. J., Derwent, R. G., Hauglustaine, D. A., Horowitz, L. W., Jacob, D. J.,
11 Johnson, M., Law, K. S., Mickley, L. J., Muller, J.-F., Plantevin, P.-H., Pyle, J. A., Rogers, H.
12 L., Stevenson, D. S., Sundet, J. K., van Weele, M., and Wild, O.: Radiative forcing in the 21st
13 century due to ozone changes in the troposphere and the lower stratosphere. *J. Geophys. Res.*,
14 108:4292, doi:10.1029/2002JD002624, 2003.

15 Hilboll, A., Richter, A., and Burrows, J. P.: Long-term changes of tropospheric NO₂ over
16 megacities derived from multiple satellite instruments, *Atmos. Chem. Phys.*, 13, 4145-4169,
17 doi:10.5194/acp-13-4145-2013, 2013.

18 Hudman, R. C., Jacob, D. J., Cooper, O. R., Evans, M. J., Heald, C. L., Park, R. J.,
19 Fehsenfeld, F., Flocke, F., Holloway, J., Hübler, G., Kita, K., Koike, M., Kondo, Y., Neuman,
20 A., Nowak, J., Oltmans, S., Parrish, D., Roberts, J. M., and Ryerson, T.: Ozone production in
21 transpacific Asian pollution plumes and implications for ozone air quality in California, *J.*
22 *Geophys. Res.*, 109, D23S10, doi:10.1029/2004JD004974, 2004.

23 Jacob, D. J., Logan, J. A., and Murti, P. P.: Effect of rising Asian emissions on surface ozone
24 in the United States, *J. Geophys. Res.*, 26(14), 2175–2178, 1999.

25 Jaffe, D., and Ray, J.: Increase in surface ozone at rural sites in the western US, *Atmos.*
26 *Environ.*, 41(26), 5452–5463, doi:10.1016/j.atmosenv.2007.02.034, 2007.

27 Jiang, Z., Worden, J. R., Jones, D. B. A., Lin, J.-T., Verstraeten, W. W., and Henze, D. K.:
28 Constraints on Asian ozone using Aura TES, OMI and Terra MOPITT, *Atmos. Chem. Phys.*,
29 15, 99-112, doi:10.5194/acp-15-99-2015, 2015.

1 Kulawik, S. S., Worden, J., Eldering, A., Bowman, K., Gunson, M., Osterman, G. B., Zhang,
2 L., Clough, S. A., Shephard, M. W., and Beer, R.: Implementation of cloud retrievals for
3 Tropospheric Emission Spectrometer (TES) atmospheric retrievals: part 1. Description and
4 characterization of errors on trace gas retrievals, *J. Geophys. Res.*, 111, D24204,
5 doi:10.1029/2005JD006733, 2006.

6 Lee, Y. C., Shindell, D. T., Faluvegi, G., Wenig, M., Lam, Y. F., Ning, Z., Hao, S., and Lai,
7 C. S.: Increase of ozone concentrations, its temperature sensitivity and the precursor factor in
8 South China, *Tellus B* 66, doi:10.3402/tellusb.v66.23455, 2014.

9 Lin, M., Fiore, A. M., Horowitz, L. W., Cooper, O. R., Naik, V., Holloway, J., Johnson, B. J.,
10 Middlebrook, A. M., Oltmans, S. J., Pollack, I. B., Ryerson, T. B., Warner, J. X.,
11 Wiedinmyer, C., Wilson, J., and Wyman, B.: Transport of Asian ozone pollution into surface
12 air over the western United States in spring, *J. Geophys. Res.*, 117(D21),
13 doi:10.1029/2011JD016961, 2012.

14 [Lin, M., Horowitz, L.W., Oltmans, S. J., Fiore, A. M., and Fan, S.: Tropospheric ozone trends](#)
15 [at Mauna Loa Observatory tied to decadal climate variability, *Nature Geosci.* 7, 136-143,](#)
16 [2014.](#)

17 Neu, J. L., Flury, T., Manney, G. L., Santee, M. L., Livesey, N. J., and Worden, J.:
18 Tropospheric ozone variations governed by changes in stratospheric circulation, *Nat. Geosci.*,
19 doi:10.1038/ngeo2138, 2014.

20 Oetjen, H., Payne, V. H., Kulawik, S. S., Eldering, A., Worden, J., Edwards, D. P., Francis,
21 G. L., Worden, H. M., Clerbaux, C., Hadji-Lazarou, J., and Hurtmans, D.: Extending the
22 satellite data record of tropospheric ozone profiles from Aura-TES to MetOp-IASI:
23 characterisation of optimal estimation retrievals, *Atmos. Meas. Tech.*, 7(12), 4223–4236,
24 doi:10.5194/amt-7-4223-2014, 2014.

25 Parrish, D. D., Millet, D. B., and Goldstein, A. H.: Increasing ozone in marine boundary layer
26 inflow at the west coasts of North America and Europe, *Atmos. Chem. Phys.*, 9, 1303-1323,
27 doi:10.5194/acp-9-1303-2009, 2009.

28 Reidmiller, D. R., Fiore, A. M., Jaffe, D. A., Bergmann, D., Cuvelier, C., Dentener, F. J.,
29 Duncan, B. N., Folberth, G., Gauss, M., Gong, S., Hess, P., Jonson, J. E., Keating, T., Lupu,
30 A., Marmer, E., Park, R., Schultz, M. G., Shindell, D. T., Szopa, S., Vivanco, M. G., Wild,

1 O., and Zuber, A.: The influence of foreign vs. North American emissions on surface ozone in
2 the US, *Atmos. Chem. Phys.*, 9, 5027-5042, doi:10.5194/acp-9-5027-2009, 2009.

3 Safieddine, S., Clerbaux, C., George, M., Hadji-Lazaro, J., Hurtmans, D., Coheur, P.-F.,
4 Wespes, C., Loyola, D., Valks, P., and Hao, N.: Tropospheric ozone and nitrogen dioxide
5 measurements in urban and rural regions as seen by IASI and GOME-2, *J. Geophys. Res.*
6 *Atmos.*, 118, 10, 555–10, 566, doi:10.1002/jgrd.50669, 2013.

7 Singh, H. B., Brune, W. H., Crawford, J. H., Flocke, F., and Jacob, D. J.: Chemistry and
8 transport of pollution over the Gulf of Mexico and the Pacific: spring 2006 INTEX-B
9 campaign overview and first results, *Atmos. Chem. Phys.*, 9, 2301-2318, doi:10.5194/acp-9-
10 2301-2009, 2009.

11 Stevenson, D., Dentener, F. J., Schultz, M. G., Ellingsen, K., van Noije, T. P. C., Wild, O.,
12 Zeng, G., Amann, M., Atherton, C. S., Bell, N., Bergmann, D. J., Bey, I., Butler, T., Cofala,
13 J., Collins, W. J., Derwent, R. G., Doherty, R., Drevet, J., Eskes, H. J., Fiore, A. M., Gauss,
14 M., Hauglustaine, D. A., Horowitz, L. W., Isaksen, I. S. A., Krol, M. C., Lamarque, J. F.,
15 Lawrence, M. G., Montanaro, V., Muller, J. F., Pitari, G., Prather, M. J., Pyle, J. A., Rast, S.,
16 Rodriguez, J. M., Sanderson, M. G., Savage, N. H., Shindell, D. T., Strahan, S. E., Sudo, K.,
17 and Szopa, S.: Multi-model ensemble simulations of present-day and nearfuture tropospheric
18 ozone, *J. Geophys. Res.*, 111, D08301, doi:10.1029/2005JD006338, 2006.

19 Tanimoto, H., Ohara, T., and Uno, I.: Asian anthropogenic emissions and decadal trends in
20 springtime tropospheric ozone over Japan: 1998–2007, *Geophys. Res. Lett.*, 36, L23802,
21 doi:10.1029/2009GL041382, 2009

22 van der A, R. J., Eskes, H. J., Boersma, K. F., van Noije, T. P. C., Van Roozendaal, M., De
23 Smedt, I., Peters, D. H. M. U., and Meijer, E. W.: Trends, seasonal variability and dominant
24 NO_x source derived from a ten year record of NO₂ measured from space, *J. Geophys. Res.*,
25 113, D04302, doi:10.1029/2007JD009021, 2008

26 Verstraeten, W. W., Boersma, K. F., Zörner, J., Allaart, M. A. F., Bowman, K. W., and
27 Worden, J. R.: Validation of six years of TES tropospheric ozone retrievals with ozonesonde
28 measurements: implications for spatial patterns and temporal stability in the bias, *Atmos.*
29 *Meas. Tech.*, 6(5), 1413–1423, doi:10.5194/amt-6-1413-2013, 2013.

1 Verstraeten, W. W., Neu, J. L., Williams, J. E., Bowman, K. W., Worden, J. R., and Boersma,
2 K. F.: Rapid increases in tropospheric ozone production and export from China, *Nat. Geosci.*,
3 8, 690-695, 10.1038/ngeo2493, 2015.

4 Wang, Y., Konopka, P., Liu, Y., Chen, H., Müller, R., Plöger, F., Riese, M., Cai, Z., and Lü,
5 D.: Tropospheric ozone trend over Beijing from 2002–2010: ozonesonde measurements and
6 modeling analysis, *Atmos. Chem. Phys.*, 12, 8389-8399, doi:10.5194/acp-12-8389-2012,
7 2012.

8 Wild, O., and Akimoto, H.: Intercontinental transport of ozone and its precursors in a three-
9 dimensional global CTM, *J. Geophys. Res.*, 106(D21), 27729–27744, 2001.

10 Worden, H. M., Deeter, M. N., Frankenberg, C., George, M., Nichitiu, F., Worden, J., Aben,
11 I., Bowman, K. W., Clerbaux, C., Coheur, P.-F., de Laat, A. T. J., Detweiler, R., Drummond,
12 J. R., Edwards, D. P., Gille, J. C., Hurtmans, D., Luo, M., Martínez-Alonso, S., Massie, S.,
13 Pfister, G., and Warner, J. X.: Decadal record of satellite carbon monoxide observations,
14 *Atmos. Chem. Phys.*, 13(2), 837–850, doi:10.5194/acp-13-837-2013, 2013.

15 Worden, H. M., Bowman, K. W., Worden, J. R., Eldering, A., and Beer, R.: Satellite
16 measurements of the clear-sky greenhouse effect from tropospheric ozone, *Nat. Geosci.*, 1(5),
17 305–308, doi:10.1038/ngeo182, 2008

18 Worden, J., Kulawik, S. S., Shepard, M., Clough, S., Worden, H., Bowman, K., and Goldman,
19 A.: Predicted errors of tropospheric emission spectrometer nadir retrievals from spectral
20 window selection, *J. Geophys. Res.*, 109(D9), D09308, doi:10.1029/2004JD004522, 2004.

21 Worden, J., Jones, D. B. A., Liu, J., Parrington, M., Bowman, K., Stajner, I., Beer, R., Jiang,
22 J., Thouret, V., Kulawik, S., Li, J.-L. F., Verma, S., and Worden, H.: Observed vertical
23 distribution of tropospheric ozone during the Asian summertime monsoon, *J. Geophys. Res.*,
24 114(D13), D13304, doi:10.1029/2008JD010560, 2009.

25 Young, P. J., Archibald, A. T., Bowman, K. W., Lamarque, J.-F., Naik, V., Stevenson, D. S.,
26 Tilmes, S., Voulgarakis, A., Wild, O., Bergmann, D., Cameron-Smith, P., Cionni, I., Collins,
27 W. J., Dalsøren, S. B., Doherty, R. M., Eyring, V., Faluvegi, G., Horowitz, L. W., Josse, B.,
28 Lee, Y. H., MacKenzie, I. A., Nagashima, T., Plummer, D. A., Righi, M., Rumbold, S. T.,
29 Skeie, R. B., Shindell, D. T., Strode, S. A., Sudo, K., Szopa, S., and Zeng, G.: Pre-industrial
30 to end 21st century projections of tropospheric ozone from the Atmospheric Chemistry and

1 Climate Model Intercomparison Project (ACCMIP), *Atmos. Chem. Phys.*, 13, 2063–2090,
2 doi:10.5194/acp-13-2063-2013, 2013.

3 Zhang, L., Jacob, D., Boersma, K., Jaffe, D., Olson, J., Bowman, K., Worden, J., Thompson,
4 A., Avery, M., and Cohen, R.: Transpacific transport of ozone pollution and the effect of
5 recent Asian emission increases on air quality in North America: an integrated analysis using
6 satellite, aircraft, ozonesonde, and surface observations, *Atmos. Chem. Phys.*, 8(20), 6117–
7 6136, 2008.

8 Zhang, Q., Streets, D. G., Carmichael, G. R., He, K. B., Huo, H., Kannari, A., Klimont, Z.,
9 Park, I. S., Reddy, S., Fu, J. S., Chen, D., Duan, L., Lei, Y., Wang, L. T., and Yao, Z. L.:
10 Asian emissions in 2006 for the NASA INTEX-B mission, *Atmos. Chem. Phys.*, 9, 5131–
11 5153, doi:10.5194/acp-9-5131-2009, 2009.

12 Zhou, D. K., Larar, A. M., Liu, X., Smith, W. L., Strow, L. L., Yang, P., Schlüssel, P., and
13 Calbet, X.: Global Land Surface Emissivity Retrieved From Satellite Ultraspectral IR
14 Measurements, *IEEE T. Geosci. Remote*, 49, 1277–1290, doi:10.1109/tgrs.2010.2051036,
15 2011.

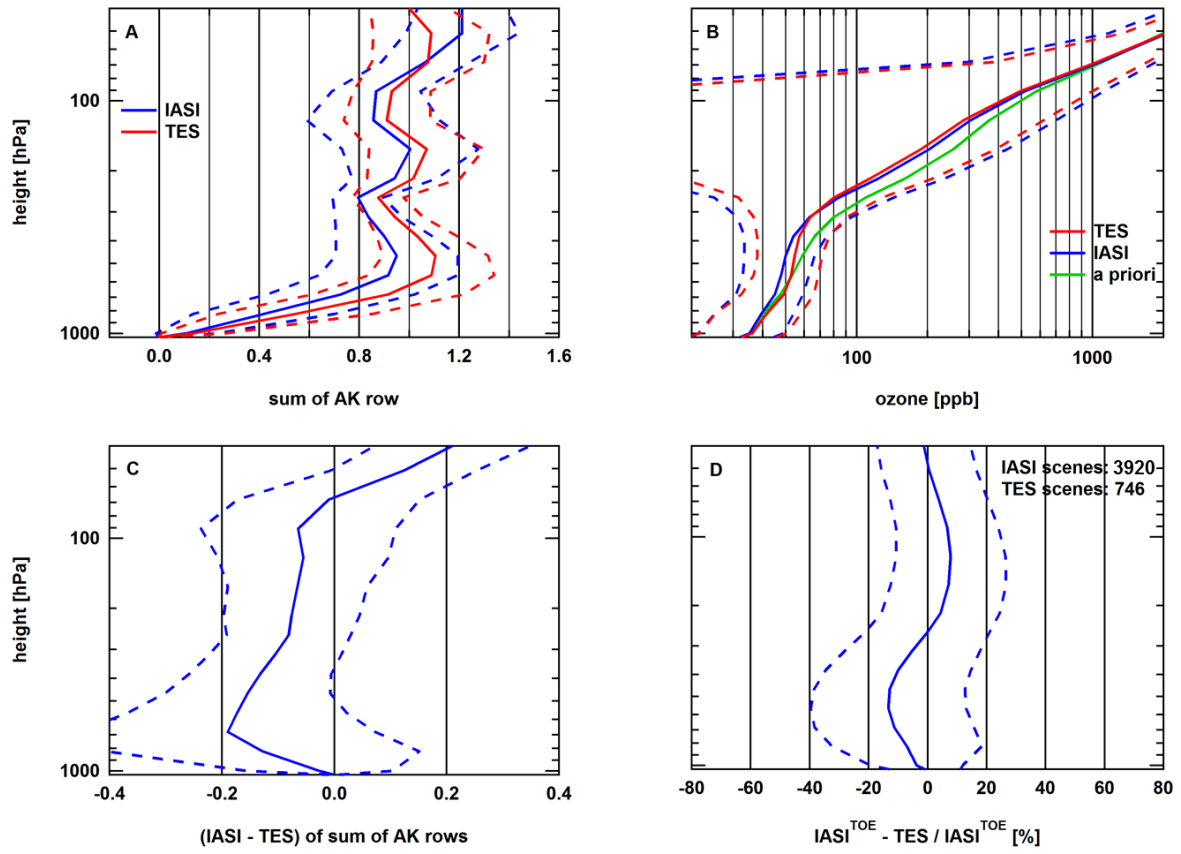
16

1

	N	$Peak (ppb)$	$FWHM (ppb)$	R^2
Spring	630	-1.7 ± 0.3	16.5	0.930
Summer	1450	-4.9 ± 0.3	19.1	0.954
Autumn	397	-4.1 ± 0.4	15.4	0.897
Winter	1443	-4.1 ± 0.1	16.4	0.968
Northern high latitudes	58	-7.0 ± 0.3	3.9	0.448
Northern midlatitudes	1567	-4.6 ± 0.2	24.7	0.953
Tropics	1714	-3.4 ± 0.1	14.7	0.983
Southern midlatitudes	581	-4.5 ± 0.4	17.2	0.904
all	3920	-3.9 ± 0.2	17.6	0.988

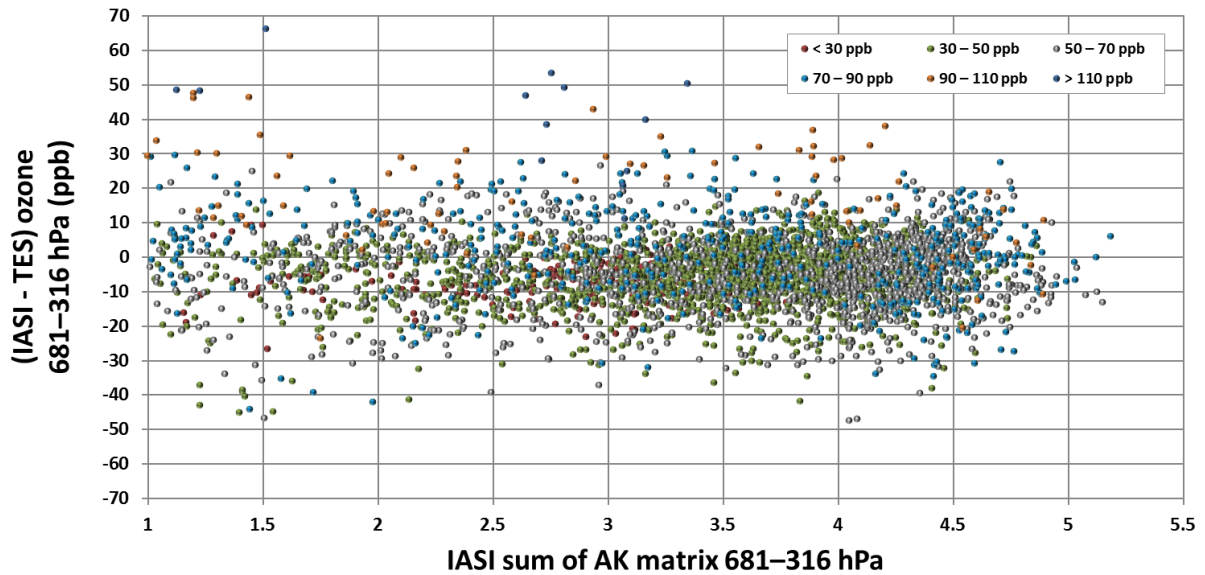
2 Table 1. Results for the Gaussian fit through the IASI-TES frequency distribution for different
3 seasons and for different latitude bands. The latitude bands were separated by the polar circle
4 and the tropics of cancer. Please note that TES measured only between 70°N and 50°S
5 latitude.

6

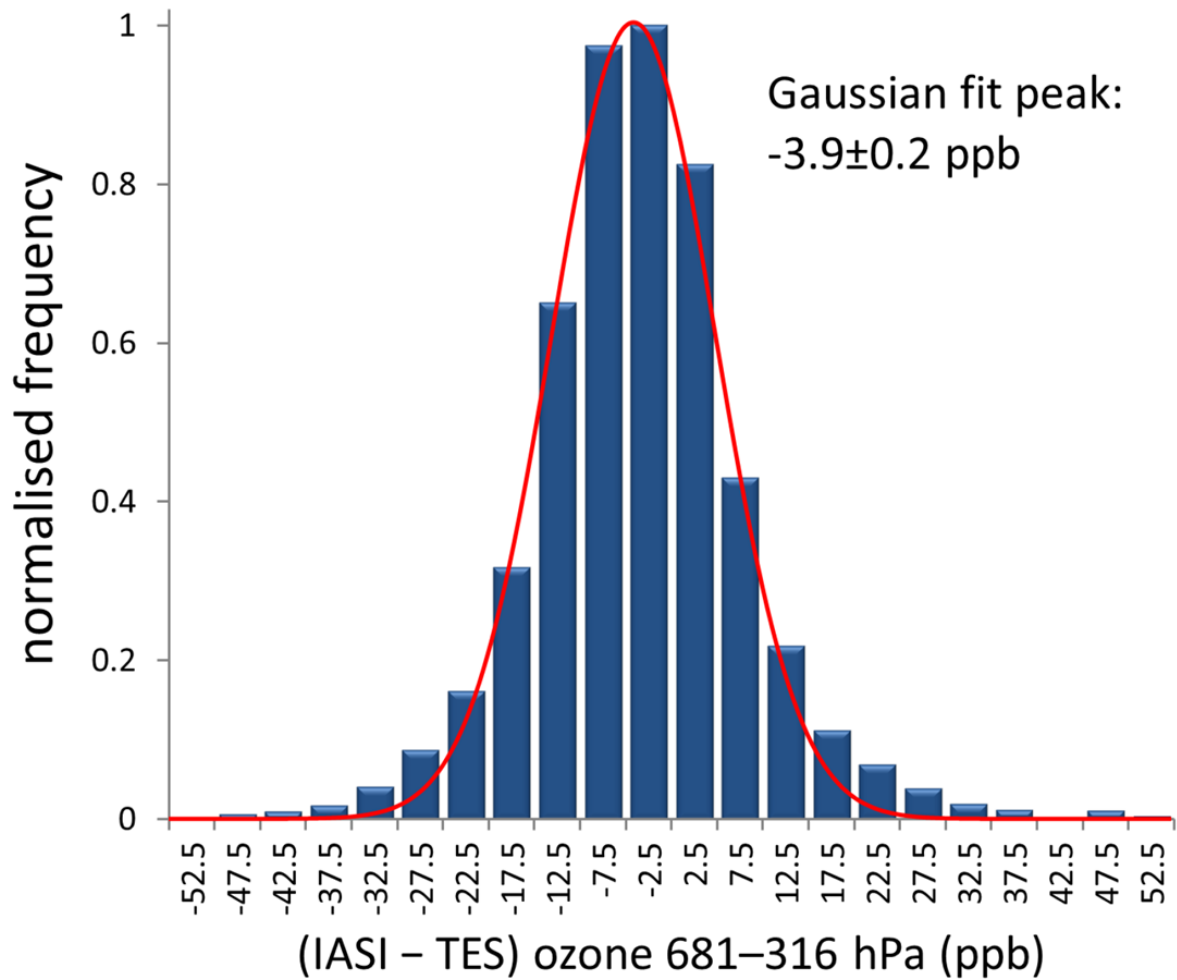


1
 2 Figure 1. Ozone profiles (panel B) and vertical sensitivities (panel A) for TES and IASI-TOE,
 3 respectively. Also shown are the differences (panel C and D). Solid lines are the mean values
 4 and dashed lines the standard deviations.

5



1
 2 Figure 2. Differences between IASI-TOE and TES 681–316 hPa average ozone mixing ratio
 3 as a function of the sum of the IASI-TOE AK matrix in the same pressure range. The [size of](#)
 4 [the markers' colour is proportional to](#) the IASI-TOE ozone mixing ratio [bins as](#)
 5 [annotaed in the legend](#). The offset between IASI-TOE and TES does neither depend on the
 6 measurement sensitivity nor the ozone mixing ratio.
 7



1

2 Figure 3. Normalised frequency distribution of the offset of the data of Fig. 2. The distribution
 3 of the difference between TES and IASI-TOE follows roughly a Gaussian function with the
 4 maximum at (-3.9 ± 0.2) ppb.

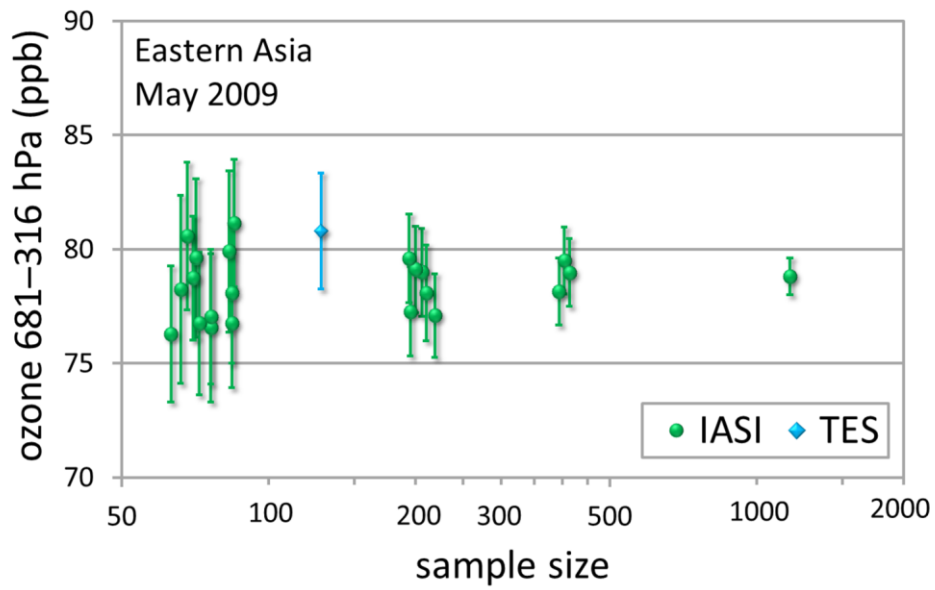
5



1

2 Figure 4. Regions of interest, Eastern Asia (corner points: [41.5°N, 116°E], [30°N, 102.5°E],
3 [20°N, 102.5°E], [20°N, 123°E], [41.5°N, 116°E]), Western US (box between 30°N and
4 50°N, 125°W and 100°W), and Europe (box between 40°N and 55°N, 10°W and 25°E).

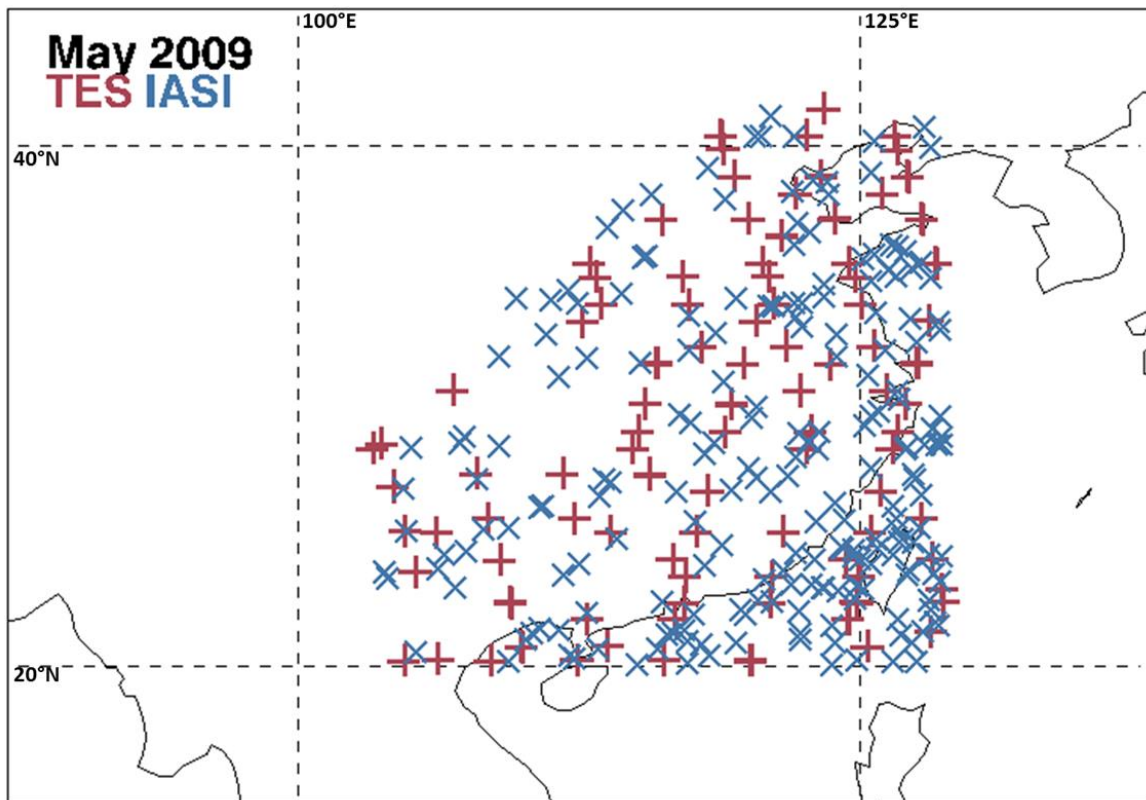
5



1

2 Figure 5. Monthly mean ozone for randomly selected IASI scenes within the Eastern Asia
 3 ROI for May 2009. IASI-TOE data has been offset-corrected. A sample of 200 IASI scenes is
 4 deemed sufficient for an uncertainty of 1.9 ppb or better for an area the size of the Eastern
 5 Asia box.

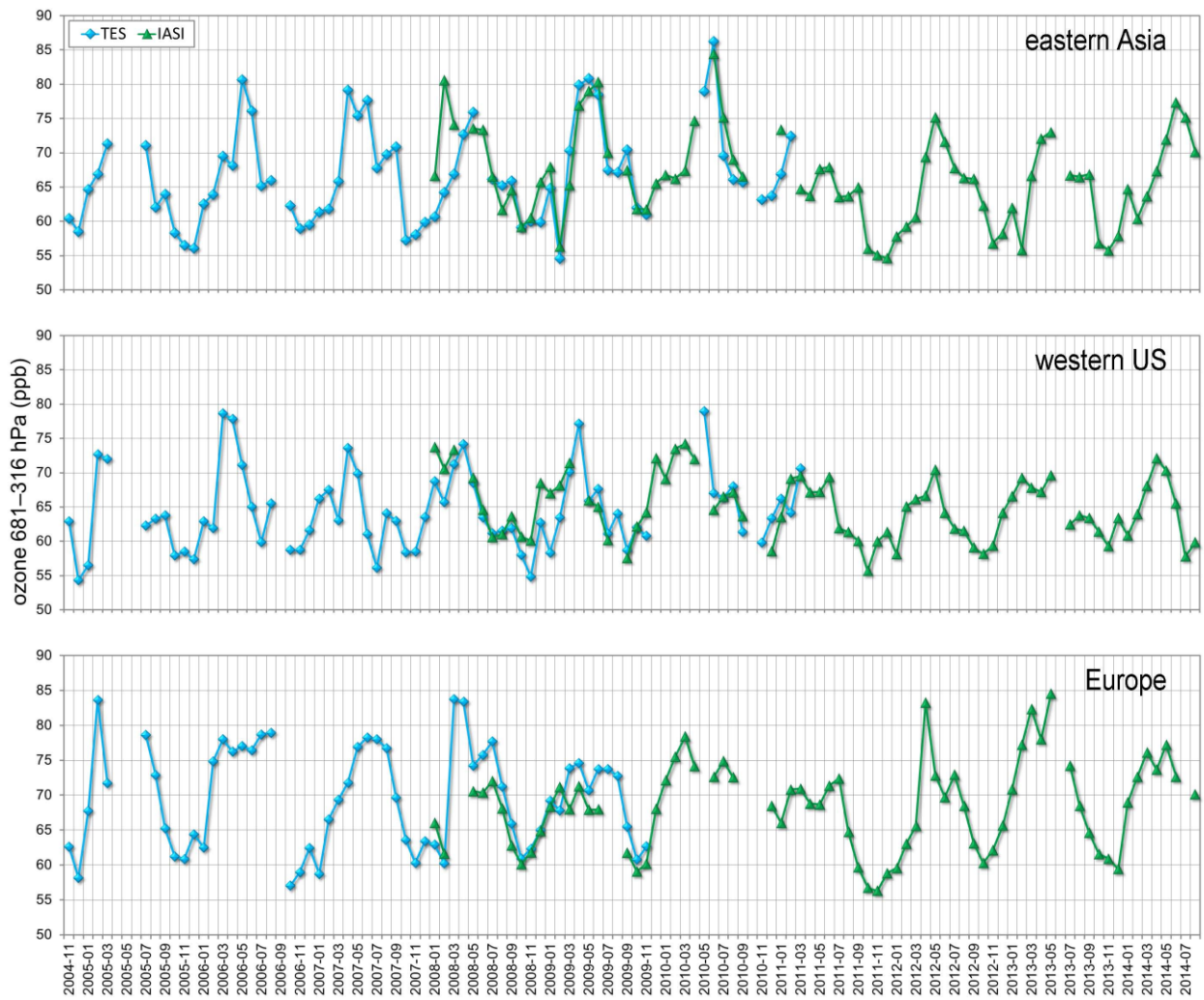
6



1

2 Figure 6. An example for the spatial distribution for 206 IASI and 128 TES data points.

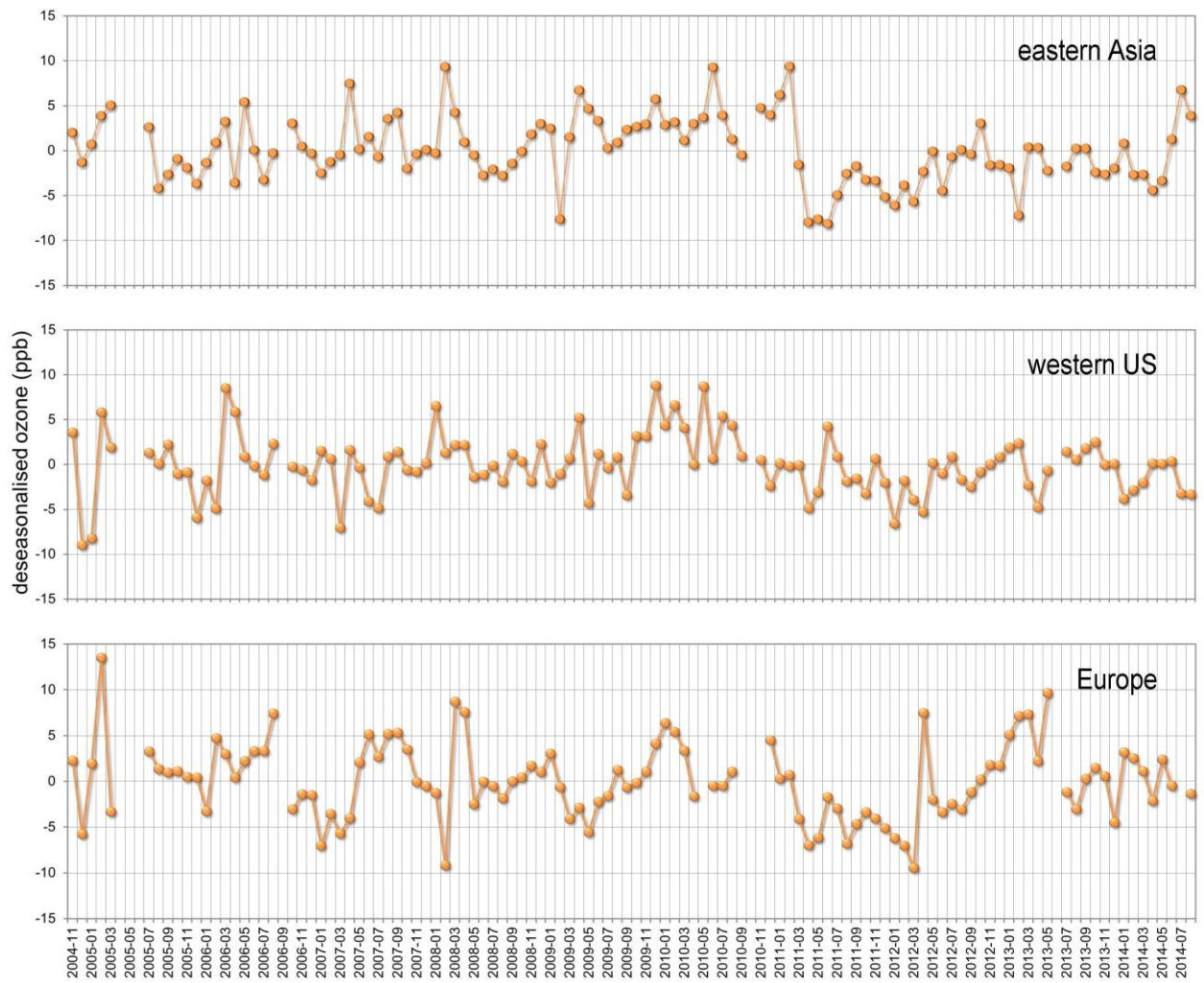
3



1

2 Figure 7. Time series of partial column averaged ozone for the 3 ROIs. IASI-TOE monthly
 3 means have been adjusted by a constant value of +3.9 ppb.

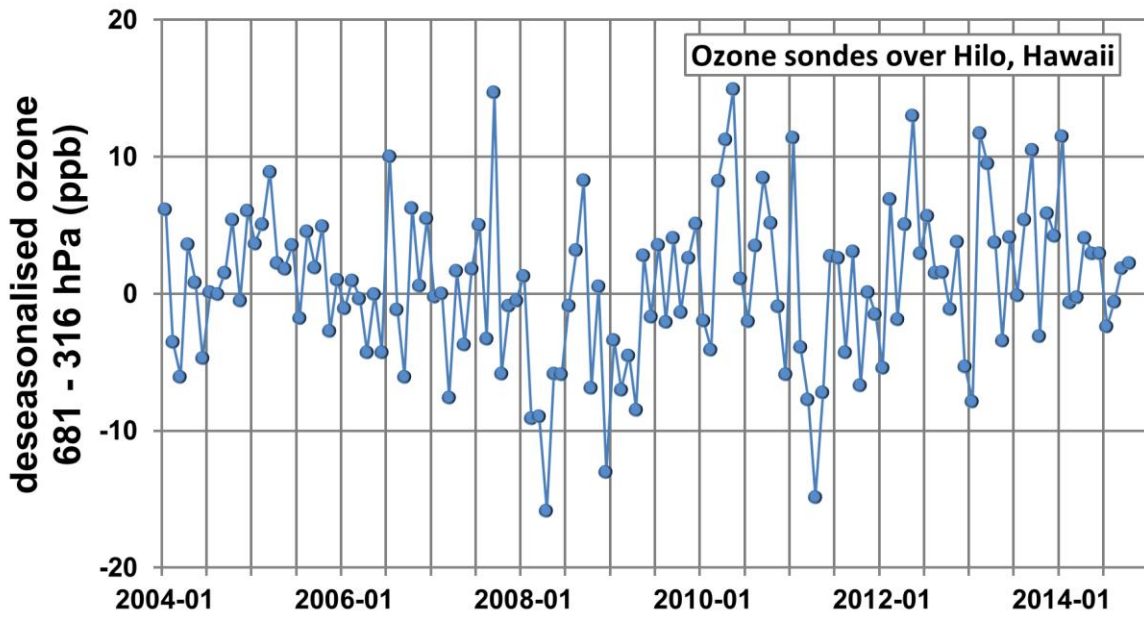
4



1

2 Figure 8. Deseasonalised joint time series for TES and IASI-TOE for the data from Fig. 7.

3

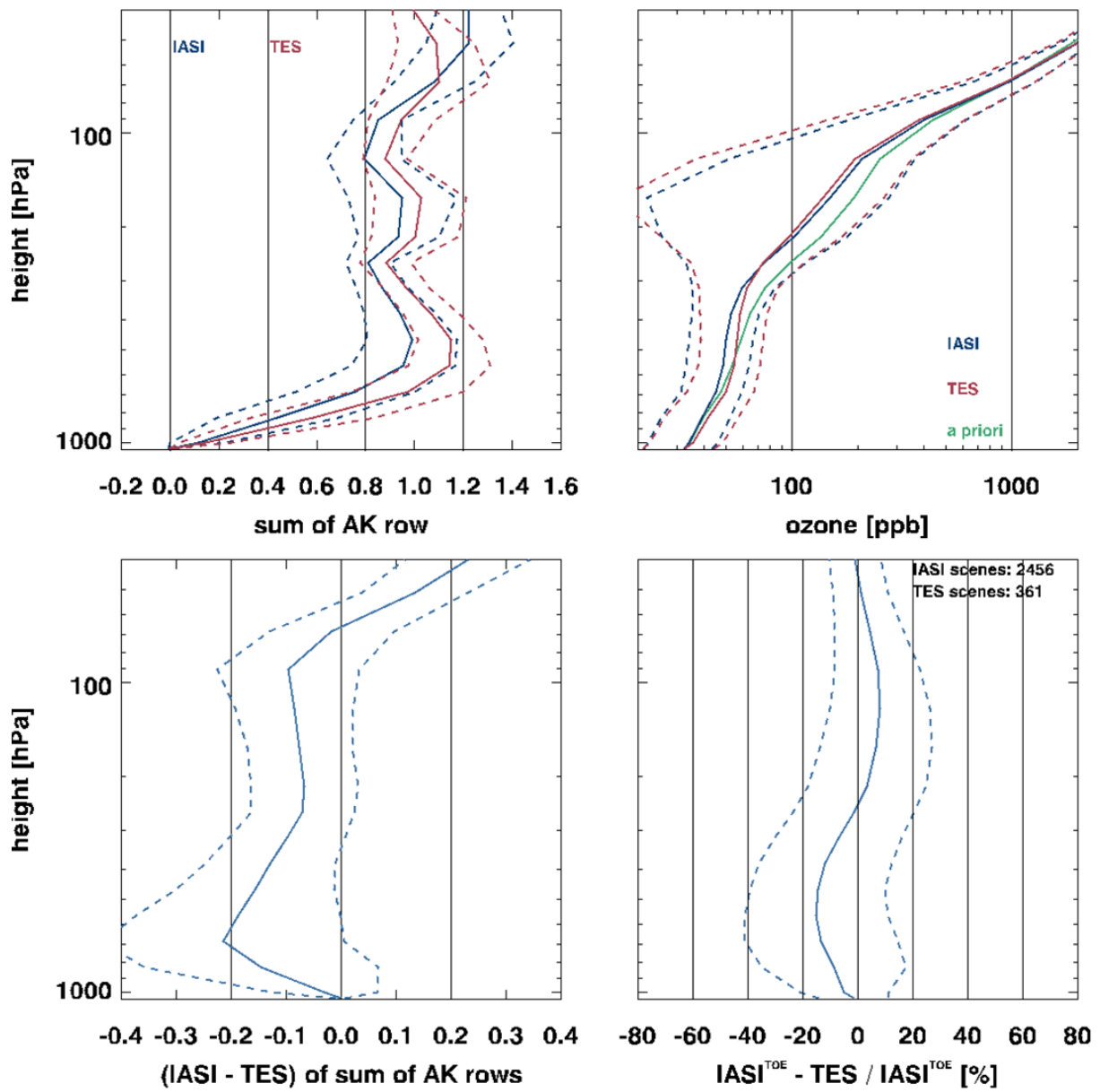


1

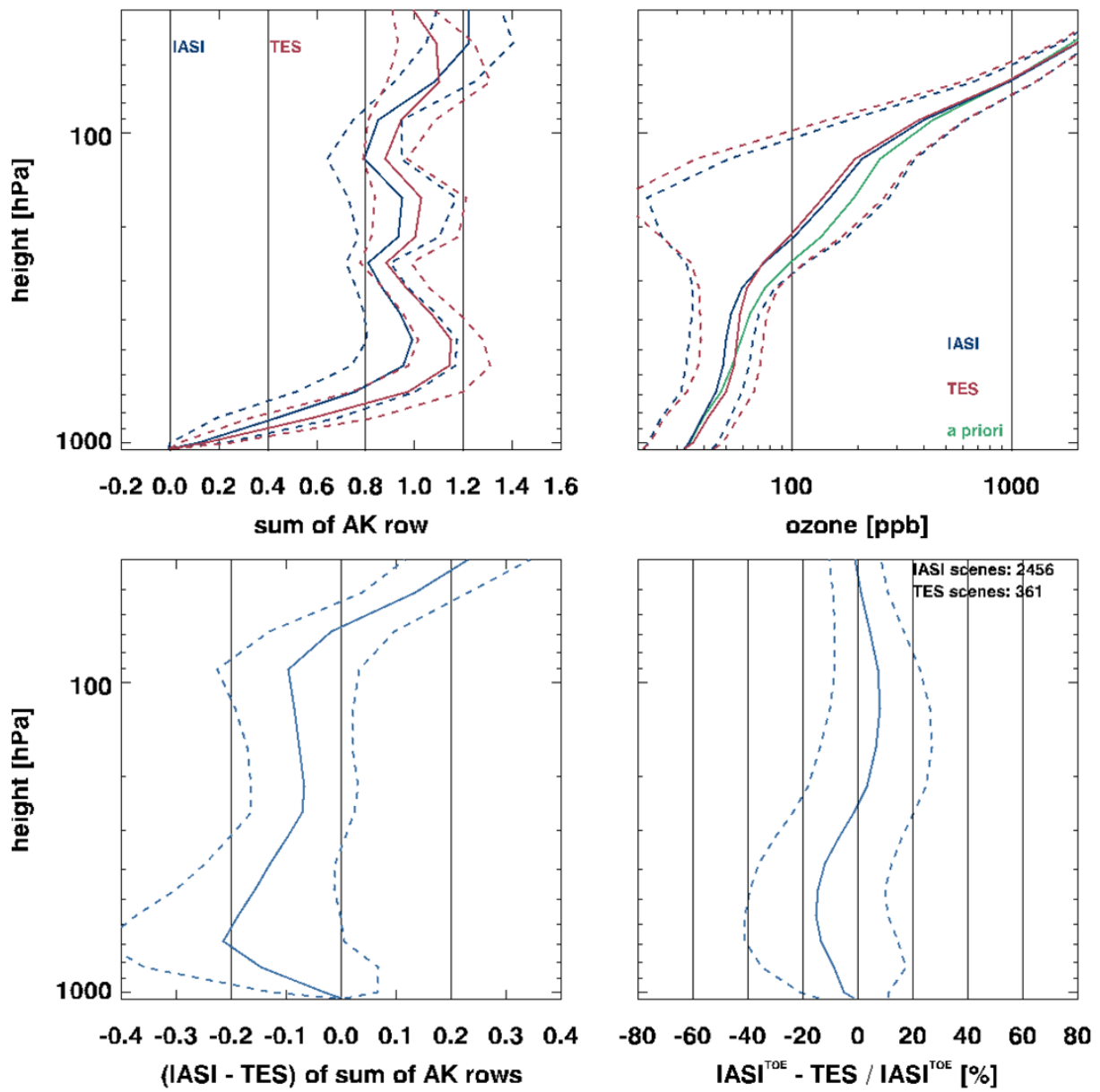
2 Figure 9. Deseasonalised time series of ozone measured by sondes in the pressure range of
 3 681–316 hPa over Hilo, Hawaii.

4

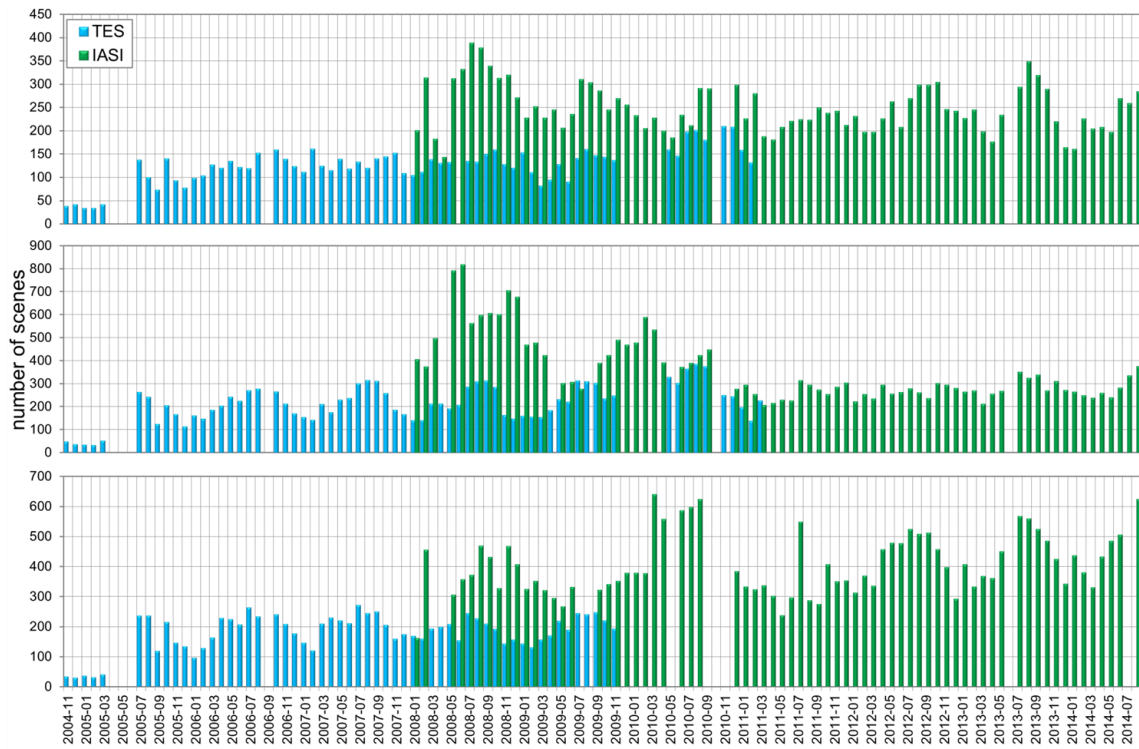
5



- 1
- 2 Figure S1. As Fig. 1 but for the August GS only.
- 3



1
2 Figure S1. As Fig. 1 but for the November GS only.
3



1
 2 Figure S3. Number of satellite data points included for the calculation of the monthly mean
 3 ozone for Fig. 7.